Journal of Power Sources 269 (2014) 284–292

Contents lists available at ScienceDirect

Journal of Power Sources

journal homepage: www.elsevier.com/locate/jpowsour

Self-powered wastewater treatment for the enhanced operation of a facultative lagoon

Timothy Ewing [a], Jerome T. Babauta [a], Erhan Atci [a], Nghia Tang [b], Josue Orellana [b], Deukhyoun Heo [b], Haluk Beyenal [a, *]

[a] The Gene and Linda Voiland School of Chemical Engineering and Bioengineering, Washington State University, Pullman, WA 99163, USA
[b] School of Electrical Engineering and Computer Science, Washington State University, Pullman, WA 99163, USA

HIGHLIGHTS

- A self-powered lagoon treatment system was developed.
- The designed self-powered system operated autonomously for more than 12 months.
- This is the first demonstration of a microbial fuel cell powering a self-sustainable wastewater treatment system.

GRAPHICAL ABSTRACT

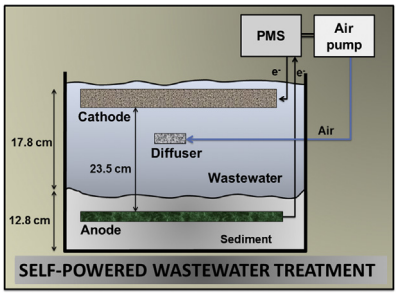

ARTICLE INFO

Article history:
Received 21 February 2014
Received in revised form
27 May 2014
Accepted 21 June 2014
Available online 7 July 2014

Keywords:
Self-powered
Power management system
Wastewater treatment
Lagoon
Microbial fuel cell
Self-starting

ABSTRACT

The goal of this study was to harness the redox gradients in facultative lagoons using a lagoon microbial fuel cell (LMFC) to enhance autonomously the delivery of oxygen to the lagoon through aeration and mixing by operating an air pump. To enhance the usability of the low power generated by the LMFC, a power management system (PMS) was used to harvest power continually while only operating the air pump intermittently. Here we demonstrate the LMFC as an alternative energy source for self-powered wastewater treatment systems by treating both artificial wastewater and dairy wastewater in large laboratory-scale simulated lagoons. For comparison, we also used a lagoon treatment system without self-aeration. We show that the integrated LMFC and PMS system was able to improve chemical oxygen demand (COD) removal time by 21% for artificial wastewater and by 54% for dairy wastewater. The LMFC-PMS wastewater treatment system operated for over a year and proved to be robust and provide a measure of sustainability. The LMFC-PMS combination offers an innovative and low-tech approach to increasing the capacity of lagoons for rural communities. We believe that the technology developed in this research is the first step towards providing sustainable self-powered wastewater treatment systems.

1. Introduction

Facultative lagoons are used in rural communities for the treatment and storage of agricultural wastewaters because they are simpler to operate and require less energy than aerated lagoons [1–5]. Commonly deep ponds, facultative lagoons naturally develop three distinct layers with oxygen concentration decreasing

* Corresponding author. Tel.: +1 509 335 6607.
E-mail address: beyenal@wsu.edu (H. Beyenal).

http://dx.doi.org/10.1016/j.jpowsour.2014.06.114
0378-7753/

by depth. Wind-aided air mixing at the surface, possibly in addition to phototrophic oxygen production from resident microorganisms, maintains an aerobic zone above both a middle facultative zone and a bottom anaerobic zone [3,6]. Aerated lagoons require constant energy input, usually in the form of mechanical surface mixing or air infusion agitation, to maintain an oxygen concentration throughout the volume and to keep suspended solids from settling. The added energy input can be advantageous, considering that aerated lagoons have a smaller footprint in the sense that they require less land than facultative lagoons [7]. This footprint is directly related to both the hydraulic retention time and the solids retention time needed to adequately treat the wastewater. Because of the variability of wastewater strength, facultative lagoon hydraulic retention times can reach 120 days or more while those of aerated lagoons can be as short as a few days [2]. Therefore a trade-off exists between the energy input and the treatment time of lagoons that can be manipulated to ensure proper wastewater treatment at the appropriate cost.

At an added cost, renewable energy sources such as solar and wind energy can be utilized to optimize lagoon wastewater treatment. Introducing active aeration utilizing renewable energy into an otherwise passive, facultative lagoon allows more agricultural wastewater to be treated using less land. Although solar and wind are possible sources of this renewable energy, they are often site-specific and seasonal, and they require substantial infrastructure not commonly found in agricultural settings. We suggest that one low-maintenance approach is to harness the redox gradient that already exists in facultative lagoons through the use of microbial fuel cell (MFC) technology; we will refer to our systems as lagoon microbial fuel cells (LMFC) [8]. The redox gradient refers to the variation in redox potential (E_h) from the aerobic zone, through the facultative zone, to both the anaerobic liquid zone and the sediment in the facultative lagoon. Typically, an excess of oxygen drives E_h to positive values in the aerobic zone. In this environment, an LMFC cathode would accept electrons via the oxygen reduction reaction [9–11]:

$$O_2 + 4H^+ + 4e^- \rightarrow 2H_2O \quad (1)$$

The presence of oxygen and possible colonization of the cathode with bacteria enhancing the oxygen reduction reaction create a sustainable biocathode [12–15]. At the other end of the gradient, several centimeters into the sediment at the bottom of the lagoon, anaerobic processes drive E_h to negative values depending on the native anaerobic respiration pathways in the sediment [16,17]. Here we assume that through microbial metabolism organic carbon oxidizes completely to carbon dioxide and releases protons and electrons according to the following reaction:

$$\text{Organic Carbon} + H_2O \rightarrow CO_2 + H^+ + e^- \quad (2)$$

Unlike the cathode, which utilizes an abiotic electrochemical pathway, the oxygen reduction reaction, the anode operates in a bioelectrochemical environment populated by a complex microbial community. This microbial community generates by-products that can be oxidized at the anode [12,18–24]. Based upon Equations (1) and (2), LMFCs are restricted to lagoon systems with both aerobic and anaerobic zones and cannot be utilized in completely anaerobic or completely aerobic lagoons (unless an alternative cathodic/anodic half reaction is used).

There are now almost innumerable demonstrations of MFCs treating various wastewaters and producing electricity in the literature [25–49]. Here the main role of the LMFC is not to treat wastewater and generate electricity but to operate an air pump that enhances wastewater treatment in an otherwise passive, facultative lagoon. To accomplish this enhanced operation, we employed a power management system (PMS). PMSs have been shown in the literature to increase the usability of the energy drawn from MFCs [10,50–61]. Although it has been reported that MFCs can produce high power (on the order of several watts m^{-2} or watts m^{-3}), to the best of our knowledge there is currently no device which can produce watt-level power unless that energy is stored for intermittent use. For example, Donovan et al. used a PMS to operate a 2.5-W wireless sensor system powered solely by an MFC generating only 3.4 mW of continuous power. This was only possible by continuously storing the energy in a capacitor and utilizing it intermittently to generate high power [54]. In this work, we follow the same strategy of harvesting energy continuously but using it intermittently. However, a new PMS needed to be developed to operate from low power generating LMFC compared to higher power generating sediment MFCs operated in rivers.

The goal of this study was to demonstrate the use of an LMFC to generate energy to run an air pump to enhance the operation of a facultative lagoon. Large laboratory-scale (83.3-L) facultative lagoons treating low-strength wastewater were used in this study. An LMFC was deployed in a lagoon with the anode buried in the anaerobic sediment and the cathode suspended in the aerobic liquid. We designed a PMS to harvest energy continuously and use it intermittently to operate an air pump. The addition of subsurface air enhanced the facultative lagoon treatment and increased chemical oxygen demand (COD) removal efficiency. We tested both artificial wastewater (AWW) and dairy wastewater (DWW). Our lagoon systems operated for more than one year in batch cycles. For a control, we used a replicate lagoon system without the aeration components. While running the experimental trials, we sampled at predetermined intervals and determined the COD and dissolved oxygen (DO) concentrations of the wastewater and open circuit potential (OCP) of the electrodes. The operation of the LMFC and the PMS were monitored autonomously using a data acquisition system. Lastly, we measured DO, pH and redox potential changes by depth in the sediment using microelectrodes.

2. Materials and methods

2.1. Lagoon microbial fuel cell and components

Fig. 1 shows a schematic diagram of the LMFC and its components. The LMFC consisted of two electrodes, an anode and a cathode, and a PMS which collected the energy and operated the air pump. For the laboratory-scale facultative lagoon, we used an 83.3-

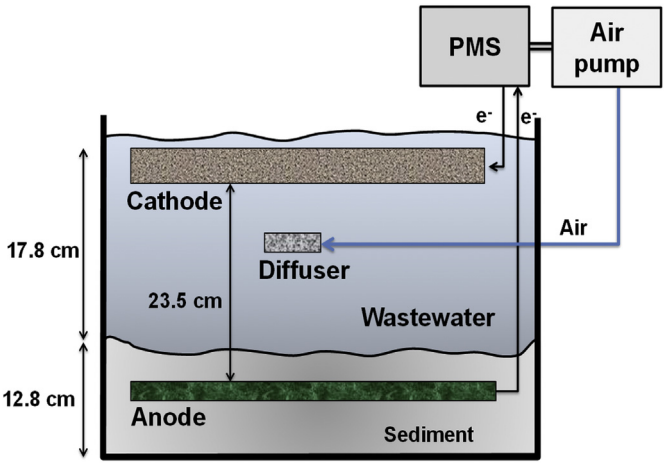

Fig. 1. Schematic diagram of the lagoon microbial fuel cell including a power management system with an integrated air pump that delivers oxygen to the wastewater.

L plastic container with a working volume of 75.7 L (Sterilite Corporation, Townsend, MA 01469, USA). The anode and the cathode were graphite felt (HP Materials Solutions, Inc., Woodland Hills, CA 91367, USA) and had projected surface areas of 0.225 m^2 and 0.674 m^2, respectively. The approximate sediment depth was 12.8 cm, and the anode was placed 7.7 cm below the wastewater/sediment interface. The depth of the wastewater was 17.8 cm, and the cathode was placed with its top just breaching the wastewater/air interface. The anode and the cathode were connected to the PMS using Grade 2, 0.635-mm-diameter Ultra-Corrosion Resistant Titanium Wire (McMaster-Carr, Los Angeles, CA 90054). Ti wires were woven into the graphite felt and secured with nylon bolts. A mechanical and solder connection to copper wire was sealed with silicone rubber to prevent water intrusion to complete the connection to the PMS. The resistances of the copper wire, Ti wire and graphite felt connections were less than 1 Ω at every point measured around each electrode. We used KPM-08A-3A air pumps (Clark Solutions, Hudson, MA 01749, USA). A diffusor placed 2.5 cm below the cathode was used to deliver subsurface air (Fig. 1).

We used an AWW and a DWW for separate experimental trials. The AWW contained 128.2 mg L^{-1} sodium acetate, 10.9 mg L^{-1} ammonium chloride, and 1.9 mg L^{-1} potassium hydrogen phosphate [62]. The COD of the AWW was adjusted to the experimentally desired value by changing the acetate concentration [62]. The initial pH of the AWW was approximately 7.1 ± 0.2. The DWW was obtained from post-fiber separated flush manure at the Knott Dairy, Pullman, WA 99163, operated by Washington State University. The initial pH of the dairy wastewater was 8.2 ± 0.2. The COD of the dairy wastewater was measured before each experiment. During the trials, the pH did not deviate significantly from the initial pH (±0.2).

We operated reactors in batch mode with various approximate COD starting values (100, 300, 500, and 1000 mg COD/L) with replication. We also used replicate control reactors, which were identical to the one shown in Fig. 1 but with the self-aeration components removed. COD was determined using Hach test kits (method 8000; Hach Company, Loveland, CO, USA). We note that the initial bulk dissolved oxygen (DO) was about half saturation. We did not find any H_2S generation in the bulk solution. We used the readily available COD reduction to represent organic carbon removal by aeration of the wastewater from both the air pump and the control. DO and pH in the bulk were monitored using a dissolved oxygen electrode (Oakton DO 110; Oakton Instruments, Vernon Hills, IL, 60061) and a pH electrode (301560.1; Denver Instrument, Bohemia, NY 11716).

The individual potentials of the anode and the cathode without self-aeration were measured against a Ag/AgCl (saturated) reference electrode and monitored at four samples per second with an Arduino Uno microcontroller board (Arduino, Ivrea, Italy, http://arduino.cc) connected to a laptop using LabVIEW© (National Instruments Corporation, Austin, TX 78759, USA). Our custom LabVIEW program displayed a real-time strip chart of potential versus time and recorded the data. When needed, polarization curves were generated using a Reference 600™ potentiostat (Gamry Instruments, Warminster PA, USA).

2.2. Power management system and aeration

A PMS was designed to harvest energy from the LMFC and intermittently operate the air pump. A block diagram of the PMS is shown in Fig. 2. The main components include energy storing devices (capacitors), a charge pump for automatic repowering of the system, two DC/DC converters, a hysteretic comparator and an n-channel MOSFET switch to control energy storage. To control the flow of energy through the PMS to the air pump, the hysteretic

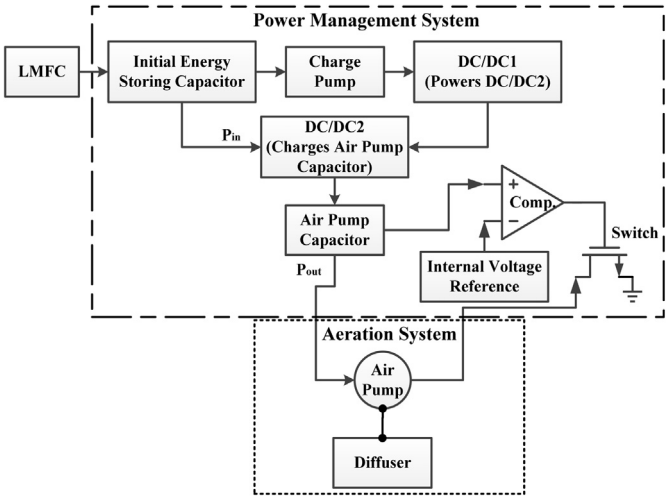

Fig. 2. Block diagram of the lagoon microbial fuel cell with power management system and aeration system.

comparator only drives the MOSFET switch closed when the potential of the air pump capacitor exceeds the preset internal voltage reference.

The energy produced by the LMFC is first stored in a 5-F ultracapacitor (Maxwell Technologies, Inc., San Diego, CA 92123, USA) called the initial energy storing capacitor (IESC). This capacitor is connected directly to the LMFC. When the capacitor reaches 320 mV, the charge pump activates the first DC-to-DC converter (DC/DC1), which provides the power to activate the second DC-to-DC converter (DC/DC2). After startup, DC/DC2 transfers energy from the IESC to a 2.5-F ultracapacitor (Maxwell Technologies, Inc., San Diego, CA 92123, USA) called the air pump capacitor (APC). When the APC potential reaches 1.3 V, the hysteretic comparator closes the MOSFET switch. The air pump is powered and runs until the APC drops below 1.2 V, at which point the switch opens. The air pump is not powered again until the next cycle. The PMS was designed with two DC-to-DC converters because the output of a single DC-to-DC converter is not sufficient to power itself and charge the APC or run the air pump directly. Thus, DC/DC1 is used to generate a 3-V output to power itself, DC/DC2, and the hysteretic comparator while DC/DC2 is used to transfer energy from the IESC to the APC. Without DC/DC1, DC/DC2 could not be started up, and the charge pump instead would need to run continuously, which would reduce the PMS efficiency. The current passed during the brief operation of the charge pump, the two DC-to-DC converters, and the hysteretic comparator is approximately 40 μA (<1% of the current from the IESC during discharge). The two-stage design of this PMS bridges the large potential and current gap between the native LMFC output and the air pump requirements. Quantitatively, the air pump draws approximately 200 mA when powered. This current magnitude cannot be provided directly by the LMFC or even by a single DC-to-DC converter since the power efficiency would be limiting. Thus, the second stage (DC/DC2 and APC) is used to accumulate energy at a higher voltage, one sufficient to run the air pump.

The PMS presented in this work implemented a charge pump and two DC/DC converters operating in parallel which was novel. The charge pump and DC/DC1 were only used to startup and power DC/DC2. The energy flow from the input to the output was through only DC/DC2. The operating principle was similar to that of the PMS by Donovan [52] except an output ultracapacitor which was used to accumulate energy at high potential to provide high power intermittently for the air pump. The structure was also similar to that of the PMS by Donovan [52] except a combination of charge pump and

DC/DC1 was used to startup and operate DC/DC2. These modifications were necessary due to lower power generation by LMFC comparing to sediment MFCs used by Donovan [52,54]. Due to the large output ultracapacitor, DC/DC2 took very long time to produce a high output voltage to power itself. Without DC/DC1 to help power DC/DC2, the charge pump would have to operate continuously, which could reduce efficiency dramatically.

We emphasize that the robustness of this PMS in its self-starting function is dependent upon the startup potential of the charge pump, which is 320 mV. The startup potential of the charge pump must be below the LMFC operating cell potential so that the IESC can activate the charge pump. In our case, allowing the IESC to cycle between 50 and 320 mV provided optimal power for the PMS [54,63]. Furthermore, the APC cycles between 1.2 and 1.3 V during steady state operation and the LMFC-PMS was self-starting and self-sustaining during all of our experimental trials. With our system there is no need for batteries or pre-charged components to use as initial energy inputs.

2.3. Characterization of the PMS

The overall power efficiency of the PMS was determined by measuring the power efficiency of DC/DC2. Based on laboratory measurements and component data sheets, it was determined that the power consumption of the charge pump, DC/DC1, and the cycling of the MOSFET switch could be ignored. To characterize the power efficiency of DC/DC2, we used a variable voltage source with an adjustable output current limit and resistive loads to control the input power. The power efficiency (η) of a DC-to-DC converter can be expressed using the following equation [54]:

$$\eta = 100 \cdot \frac{P_{out}}{P_{in}} \tag{3}$$

where P_{in} is the average power transferred into the DC-to-DC converter and P_{out} is the average power delivered by the DC-to-DC converter. During our power efficiency tests we used a resistor as a static load in place of the air pump.

Fig. 3 shows the power efficiency of DC/DC2 with an input potential of 400 mV. The input voltage, the output voltage, and the load resistor values were recorded. The input current was estimated by connecting a 1.26-Ω resistor in series with the power supply and measuring the voltage difference across it. The load was changed to adjust the output power. With the input voltage, input current, output voltage and load resistor known, the input power and output power can be calculated. From these power values, the efficiency was estimated. Only a power supply and a digital multimeter are required for these measurements. Since the power from an LMFC typically varies during operation, we also tested the efficiency of the power management system under simulated nonrhythmic conditions. A variable current supply was connected to DC/DC2 to simulate nonrhythmic charge/discharge cycles. We found that the power efficiency trend under nonrhythmic conditions did not deviate significantly from that shown in Fig. 3.

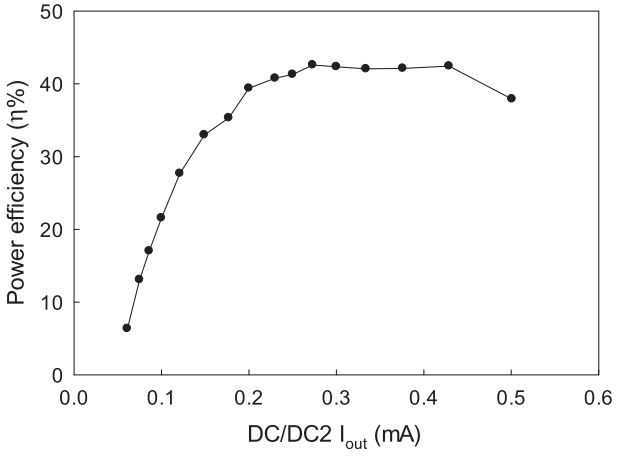

Fig. 3. Power efficiency versus output current for DC/DC2 with an input potential of 400 mV and output potential of 1.3 V.

2.4. Power generation using capacitors

The average power (P_{avg}) generation in a single-capacitor charge/discharge cycle is calculated using Equation (4) [63]:

$$P_{avg} = \frac{1}{2} \frac{C\left(V_c^2 - V_d^2\right)}{t_c - t_d} \tag{4}$$

where C is the capacitance in farads, the capacitor is charged from V_d (discharge potential) to V_c (charge potential) (volts), and $(t_c - t_d)$ is the charging time in seconds. This is the time elapsed between the capacitor being discharged (t_d) and the capacitor being charged again (t_c).

2.5. Open circuit potential measurements

Open circuit potentials are measured using a voltmeter (Keithley 6517A Electrometer/High Resistance Meter) against a Ag/AgCl reference electrode under no current conditions. If the system was operating, we simply disconnected the PMS and air pump and then measured the open circuit of the electrode after equilibrium was reached. However, if we needed to measure individual anode and cathode potentials, their potentials were simply measured against a Ag/AgCl reference electrode.

2.6. Microelectrode measurements

Dissolved oxygen (DO), redox potential and pH microelectrodes were used to characterize the gradients in the sediment. Microelectrodes with tip diameters of less than 20 μm were used in order to reduce disruption of the sediment/bulk water interface. Microelectrode construction, calibration, and measurement have been detailed elsewhere [64]. Briefly, the DO microelectrode is an amperometric sensor in which the silicone rubber membrane of the microelectrode tip is permeable to oxygen. The gold cathode in the vicinity of the silicone rubber membrane reduces oxygen, and the reduction current is a function of the dissolved oxygen concentration near the microelectrode tip. The redox potential and pH microelectrodes are potentiometric sensors. The redox potential microelectrode tip was made by electrochemically depositing platinum on a platinum microelectrode tip, resulting in a porous platinum ball with a large surface area. The redox potential microelectrode was calibrated using a standard YSI 3682 Zobell Solution (YSI Inc., Yellow Springs, OH). The pH microelectrode had a liquid ion-exchange membrane at the tip and was calibrated using standard buffer solutions (pH 4, 7, and 10) from ACROS Organics. For E_h and pH, a Keithley 6517A Electrometer/High Resistance Meter was operated as a high-resistance meter. The potential difference was read between the microelectrode tip and the reference electrode. The response time of each microelectrode was less than a few seconds.

To measure a depth profile, a microelectrode was positioned above the sediment using micromanipulators. The microelectrode was then positioned ~1000 μm from the sediment surface and

stepped down. The movement of microelectrodes was controlled by a Mercury Step motor controller PI M-230.10S Part No. M23010SX (Physik Instrumente, Auburn, MA) controlled by custom Microprofiler® software. The locations of the microelectrode tip and the surface of the sediment were observed using a stereomicroscope (Zeiss Stemi 2000 stereo-microscope). It took several minutes to complete a depth profile.

In our experiments, the LMFCs were run for over a year without any mechanical/electrical failures. Over approximately six months, replicated batch WW treatment experiments were run. During idle periods, the LMFCs continued operation but at a slower charge/discharge rate because of limited nutrient availability.

3. Results and discussion

3.1. Redox gradients at the sediment/bulk water interface

Stratification of E_h, pH, and DO across the sediment/bulk water interface is commonly observed in lagoon systems [65,66]. Since one of the requirements for the LMFC to operate effectively was that a redox gradient be established across the sediment/bulk water interface, we measured E_h, pH, and DO using microelectrodes. Fig. 4 shows the E_h, pH, and DO depth profiles at the sediment/bulk water interface. The E_h in the bulk water was oxic and approximately +0.21 $V_{Ag/AgCl}$. At 5 mm below the surface, the E_h decreased to −0.15 $V_{Ag/AgCl}$. Since E_h is also affected by local pH, we also measured pH in the sediment and showed that pH decreased minimally from approximately pH 7.8 in the bulk water to pH 7.3 at 5 mm below the surface. DO decreased from approximately 85% saturation in the bulk water to below our detection limit 1.25 mm below the sediment surface. The depth profiles of E_h, pH, and DO confirmed the redox stratification necessary to operate the LMFC in the lagoon system and suggest that any anode placed at a depth greater than ~3 mm (gray shaded area in Fig. 4) will operate under anaerobic conditions. To be certain that such conditions were met, we placed the anodes deeper into the sediment.

3.2. Open circuit potentials of the LMFC anodes and cathodes

Fig. 5 shows the development of OCP during a batch wastewater treatment cycle for both the aerated LMFC-PMS and the non-aerated control LMFC. Here OCP was obtained by temporarily disconnecting the LMFC anodes and cathodes. Control LMFC cathodes and anodes reached approximate steady values of +320 $mV_{Ag/AgCl}$ and −240 $mV_{Ag/AgCl}$, respectively. LMFC-PMS cathodes and anodes reached approximate steady values of +430 $mV_{Ag/AgCl}$ and −400 $mV_{Ag/AgCl}$, respectively. Although the LMFC-PMS and control LMFC started out at nearly identical cathode and anode OCPs, we found that the OCP of LMFC cathodes and anodes outperformed that of the control system across multiple replicates of batch cycles. A lower anodic OCP indicates more microbial reducing activity in the sludge where the anode was deployed [63,67]. The higher OCP of the cathodes indicates higher cathodic activity [63,67]. Since the equilibrium cell potential (cathode OCP−anode OCP) increased by 270 mV for the aerated LMFC-PMS systems, we suggest that there is a positive feedback loop in which LMFC electricity is fed directly back into the lagoon treatment system. This is mainly because of electrochemically active biofilm development on the electrode surface [68–71].

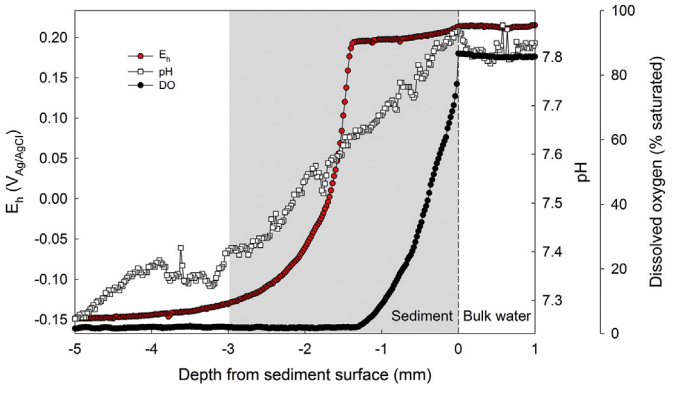

Fig. 4. Redox potential, pH, and dissolved oxygen depth profiles across the sediment–bulk water interface. Redox potential, pH, and dissolved oxygen decrease by depth indicating the existence of redox stratification in the lagoon system.

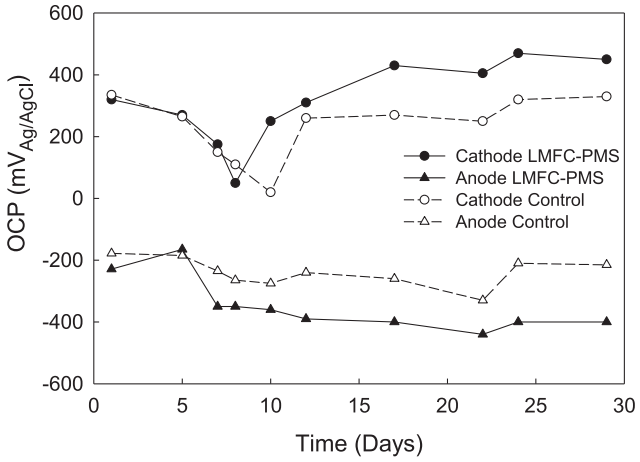

Fig. 5. Anode and Cathode open circuit potential during treatment of 100 mg COD/L AWW. Cathodes and anodes of control LMFCs (open symbols; dashed lines) were generally less positive and less negative than LMFC-PMSs (closed symbols; solid lines), respectively.

3.3. Operation of the LMFC-PMS

Fig. 6A shows an example power curve for the LMFC operating in the lagoon. The maximum power at a cell potential of 0.35 V was 1.45 mW. However, the true steady power (P_{in}) entering the PMS at DC/DC2 (Fig. 2) is shown in Fig. 6B. Losses across the PMS accumulated: P_{out} to the air pump was only ~20% of P_{in}, or 0.1 mW. Thus, the amount of power loss was about 0.4 mW, which was the difference between input power and output power. This power loss mainly came from DC/DC2. As shown in Fig. 3, at 0.1 mA and 1.3 V (or equivalently 0.13 mW), the efficiency of DC/DC2 was about 20%. The low efficiency caused by low input power, which limits the output power. To increase power efficiency and reduce losses, it is necessary to increase input power. However, the LMFCs used did not produce higher power which could improve efficiency. We should note that the pump does not operate on 0.1 mW. This is the average power (Equation (4)) outputted by the APC. We should note that power output and maximum power generated, by either LMFC or LMFC-PMS, are generally only useful as diagnostic parameters for optimization. The measured power flowing through the LMFC-PMS effectively determines the rate at which the capacitors (IESC and APC) charge/discharge. Higher power equates to quicker charge/discharge cycles across a given time period. Consequently, to determine whether the air pump and PMS are using the input power successfully, it is more useful to monitor the IESC and APC potentials during LMFC-PMS operation.

Fig. 7A gives a representative sample of the potentials of both the IESC and the APC during operation. The charge/discharge curves show a complete air pump activation cycle. Each 5–7 min charge

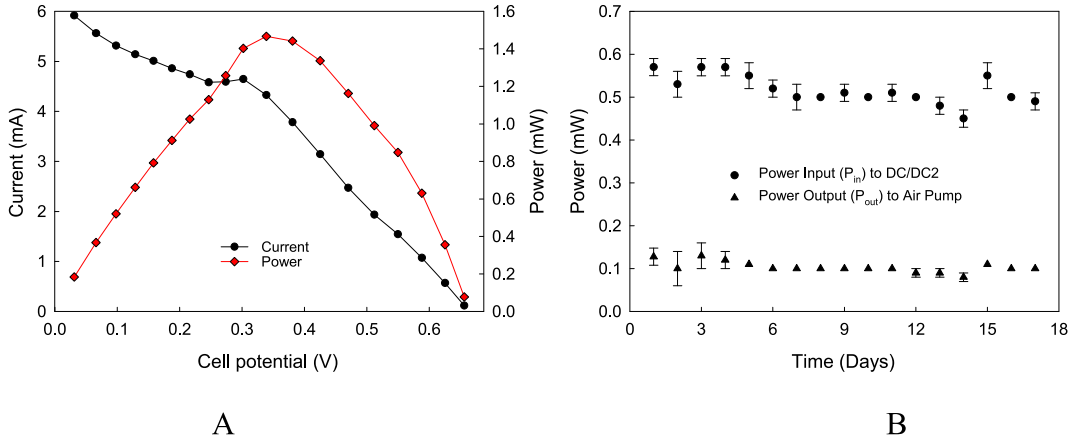

Fig. 6. A) Power curve of LMFC showing maximum power of 1.45 mW. B) Actual power output of LMFC-PMS used to power the air pump. The 0.5 mW compared to 1.45 mW shows the overestimation of sustainable power using power curves for the LMFC.

cycle of the IESC, from 50 mV (V_d) to 320 mV (V_c), activates the circuit and transfers energy to the APC in a discrete step. Each energy transfer increases the energy stored in the APC until it reaches a potential of 1.3 V and the air pump activates. The air pump operates until the output capacitor reaches 1.2 V and the next cycle starts. The cyclical charge/discharge phases are the core of the intermittent operation of the LMFC and allowed operation of the air pump with seemingly unusable power. The effect of the PMS on the LMFC is shown Fig. 7B, where the anode potentials are observed to cycle over a ~200-mV range with each operation. Since the cathode oscillations were comparatively less pronounced, the LMFC was anode-limited as described in our previous publication [72].

3.4. Effect of the self-powered air pump on COD removal

Operation of the LMFC-PMS was tested in two types of wastewater, AWW and authentic DWW, to observe a simple case and a complex case, respectively. DWW was also used because of its rural nature and likelihood of being treated in lagoon wastewater systems. Fig. 8A shows the COD concentrations and percentage COD removal over time for the LMFC-PMS and the control when they were fed with AWW. After 19 days of operation, the final COD concentration in the reactor with LMFC-PMS was 22 mg L^{-1} ± 4 mg L^{-1}; that in the control reactor was 57 mg L^{-1} ± 6 mg L^{-1}. The removal efficiencies were 93% and 62%, respectively. This is an almost 21% improvement in treatment time through the simple addition of a passive, zero-energy-input device. Fig. 8B shows the corresponding change in DO in response to the AWW loading. The immediate drop in DO to near zero on day 3 explains the slow removal rate of COD from both reactors. However, as DO recovers, the LFMC-PMS reactor recovers faster and as a result treats COD faster. The effect is two-fold: the LMFC operates better with higher DO and then aerates the reactor volume more frequently. Thus, the observations of OCP in Fig. 5 are consistent with what is shown here. Once nearly all the COD is removed, by day 19 for the LMFC-PMS reactor, the DO recovers to near its original value of 40%.

The control reactors operated successfully using an LMFC that discharged power to a pseudo-device (resistor) and treated wastewater. This was expected and an appropriate control for the PMS-LMS system since it accounted for the advantage of having COD consumed by the LMFC. The control reactors demonstrate the capability of our lagoon wastewater treatment system and suggest that if we optimize our reactors, we can achieve larger increases in COD removal for the LMFC-PMS systems as well. Huggins et al. similarly used an MFC for wastewater treatment [73]. In their study, they used an MFC reactor, a reactor with other aeration only, and a passive control (no MFC or other aeration). They found that wastewater treatment as COD removal showed significantly lower performance in their control compared to both MFC and other aeration. Fig. 8C and D, showing the change in COD was faster for the reactors fed with DWW, demonstrates this concept. Within 13

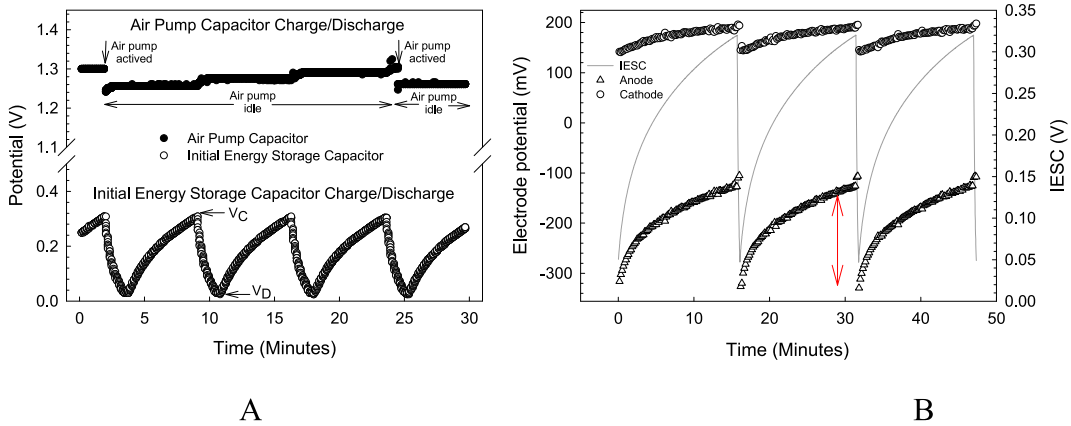

Fig. 7. (A) An example of charging and discharging cycles of the initial energy-storing capacitor and the air pump capacitor in the power management system. After several charge/discharge cycles of the initial energy-storing capacitor, the air pump capacitor discharges and activates the air pump. (B) Anode and cathode potential variation during LMFC-PMS operation.

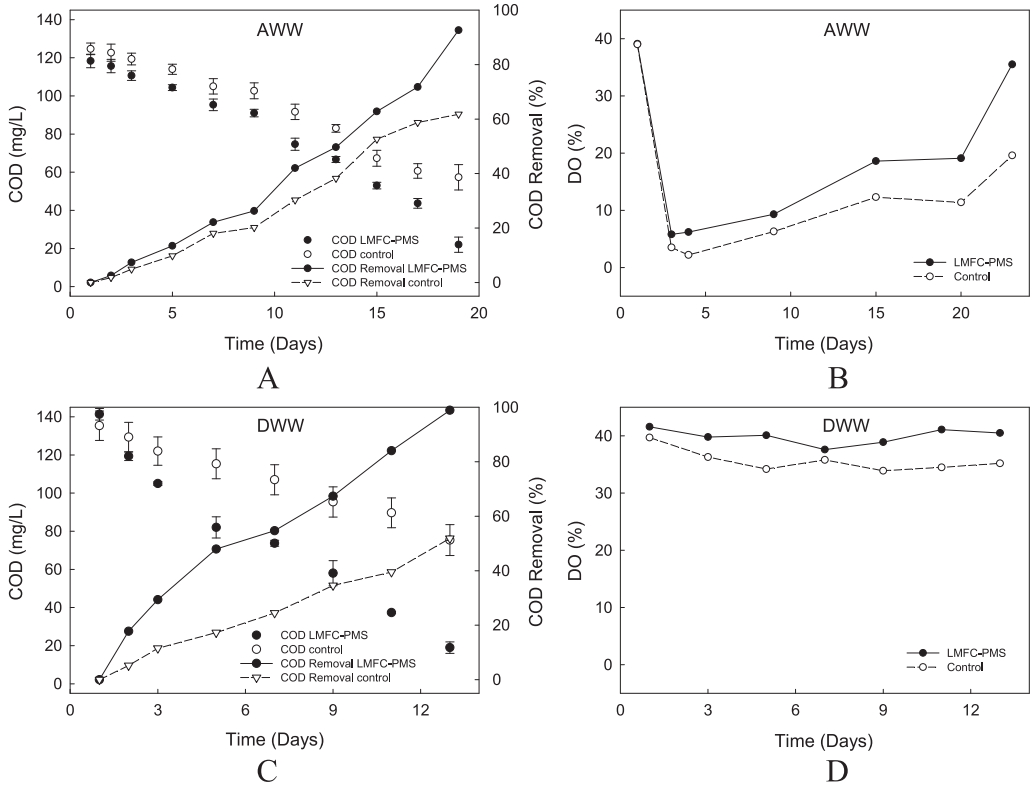

Fig. 8. COD and % COD removal over time for the LMFC-PMS and control reactors. (A) Batch treatment using AWW at 120 mg COD/L. (B) DO change in response to AWW loading. (C) Batch treatment using DWW adjusted to 140 mg COD/L. (D) DO change in response to DWW loading.

days, the final COD concentration of the LMFC-PMS was 19 mg L^{-1} ± 3 mg L^{-1} and that of the control reactor was 75 mg L^{-1} ± 8 mg L^{-1}. The removal efficiencies were 99% and 52%, respectively. For DWW treatment, the LMFC-PMS resulted in an improvement in treatment time of almost 54%. Thus, when optimized to fit a certain wastewater treatment system, the LMFC-PMS can yield large decreases in treatment time that effectively translate to more wastewater being treated in a given period. Looking at Fig. 8D, we can attribute the decrease in treatment time for the DWW to the lack of change in DO for the duration of the batch operation. The disparity between the DO responses of AWW and DWW show that management of DO is a serious concern for implementing LMFC-PMS systems. However, considering that lagoon treatment systems are constructed around the presence of DO, such a concern can be mitigated.

To confirm the importance of DO management, we increased the AWW loading to 300 mg COD/L. Fig. 9A shows the DO response to 300 mg COD/L: beyond day 4, DO remained at near-zero levels. Fig. 9B tracks the OCPs of the LMFCs in response to the change in DO and clearly shows that the cathodes of both the LMFC-PMS and the control failed. The failure occurred because DO was removed and the entire lagoon system transformed into an anaerobic lagoon system. Thus, the LMFCs were expected to fail since oxygen is required at the cathode for it to function properly. We found that the cathodes were contaminated with microbial growth in line with the absence of oxygen. Simply, our cathodes became ineffective and our LMFC stopped generating power. This is not a limitation of the LMFC-PMS system; it is only a limitation on the design of our lab-scale lagoon treatment system. When designed to tolerate higher COD, a lagoon system can still maintain the aerobic zone

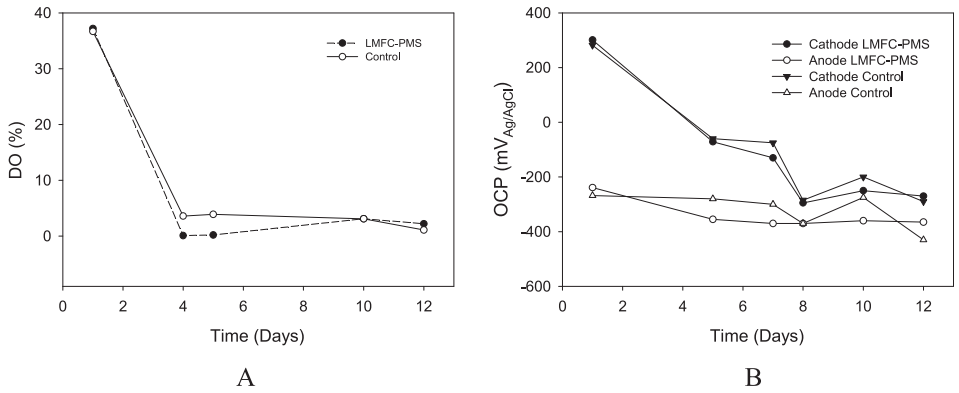

Fig. 9. (A) DO response and (B) OCP response to AWW loading of 300 mg COD/L.

which is essential to the LMFC-PMS. In our system, however, to operate an LMFC-PMS safely, the initial COD loading concentration should not be greater than 150 mg L^{-1}.

Our results demonstrate that energy harvested from an LMFC-PMS can be used to improve wastewater treatment. We found that if the initial COD loading concentration was less than 150 mg L^{-1}, the system operated successfully and transformed chemical energy in wastewater into electricity. This electricity was used to operate an air pump to aerate and improve the wastewater treatment. However, we observed decreased performance at loading concentrations greater than 150 mg COD/L and complete system failure at loading concentrations greater than 300 mg COD/L. The decreased performance and system failure were caused by cathode contamination through microbial growth. Simply, our cathodes became anodic when COD concentrations were above 300 mg L^{-1}. In practical terms, if we want to utilize energy from wastewater to power our treatment systems then we need to ensure that the cathodes remain in aerobic zones in lagoon wastewater treatment systems. As an alternative we could try to use larger electrodes to generate higher power to increase the self-powered aeration. However, we would have several challenges, in that MFCs do not scale up linearly [67]. Simply, power density does not increase linearly with electrode size. Second, making larger LMFCs would also increase the liquid volume and could lower our treatment efficiency. We believe scaling up of the system we developed here is possible but requires extensive sets of experiments using different reactor volumes, electrode sizes and operating schemes. Currently, we are in progress of developing a scalable system using these approaches. Regardless, considering that traditional passive lagoon treatments can have retention times of 120 days or more, the potential of the LMFC-PMS to reduce this time significantly opens up the possibility of increasing throughput capacity or decreasing system volume. Additionally, it is not relevant to directly compare our self-powered LMFC-PMS to an externally-powered, continuously aerated system because the continuously aerated lagoon will provide an increased COD removal rate based solely on the amount of aeration [74]. The key differences between these systems are the target application and the energy source. Our self-powered LMFC-PMS is targeted at converting existing passive lagoons, such as found extensively in agriculture, into aerated lagoons using only the energy in the wastewater. The continuously aerated system while currently favored for municipal and industrial facilities operates on unfortunately costly grid energy that could be termed parasitic [75]. Therefore, we believe that the technology developed in this research is the first step towards providing sustainable self-powered wastewater treatment systems.

4. Conclusions

In this research we found that a self-powered lagoon treatment system can treat wastewater, generate electricity and operate an air pump. This was possible because the air pump was operated intermittently using energy stored in a capacitor. The power generation by our LMFC was not able to operate the air pump continuously. By developing an intermittent energy harvesting strategy we managed to operate a self-powered lagoon treatment system. The aerated lagoon treatment system—in this case self-powered—improves COD removal time by 21% compared to a control (not aerated) for artificial wastewater. COD removal time was improved by 54% compared to a control for dairy wastewater. The LMFC-PMS performed significantly better when dairy wastewater was used than when artificial wastewater was used. The designed self-powered system operated autonomously for more than 12 months for an initial COD loading of up to 150 mg L^{-1}.

Acknowledgements

This research was supported by NSF-CAREER award #0954186 and by the U.S. Office of Naval Research (ONR), grant #N00014-09-1-0090. Beyenal acknowledges additional support from Fundamental and Applied Chemical and Biological Catalysts to Minimize Climate Change, Create a Sustainable Energy Future, and Provide a Safer Food Supply (project #WNP00807). Erhan Atci was supported by the WSU College of Engineering and Architecture, SIRE award. Nghia Tang and Josue Orellana acknowledge NSF CAREER grant ECCS-0845849 and the Korean Government (NRF-2011-220-D00084).

Nomenclature

APC	air pump capacitor
AWW	artificial wastewater
COD	chemical oxygen demand
DC/DC1	the first DC-to-DC converter
DC/DC2	the second DC-to-DC converter
DO	dissolved oxygen
DWW	dairy wastewater
IESC	initial energy-storing capacitor
LMFC	lagoon microbial fuel cell
LMFC-PMS	LMFC and PMS operated together
P_{avg}	average power
P_{in}	the average power transferred into the DC-to-DC converter
PMS	power management system
P_{out}	the average power delivered by the DC-to-DC converter
t_c	time elapse for capacitor charge
t_d	time elapsed for capacitor discharge
V_c	charge potential
V_d	discharge potential
η	power efficiency

References

[1] Dairy Australia, Effluent and Manure Management Database for the Australian Dairy Industry, 2008. Southbank Victoria 3006 Australia.
[2] Metcalf and Eddy, Wastewater Engineering: Treatment And Reuse, McGraw-Hill, 2003.
[3] US EPA, Wastewater Technology Fact Sheet: Facultative Lagoons, 2002.
[4] US EPA, s. Wastewater Technology Fact Sheet: Anaerobic Lagoon, 2002.
[5] US EPA, Wastewater Technology Fact Sheet: Aerated, Partial Mix Lagoons, 2002.
[6] M.L. Davis, Water and Wastewater Engineering: Design Principles And Practice, McGraw-Hill, 2010.
[7] US EPA, Design manual: Municipal wastewater stabilization ponds, 1983.
[8] R.A. Rozendal, H.V. Hamelers, K. Rabaey, J. Keller, C.J. Buisman, Trends Biotechnol. 26 (8) (2008) 450–459.
[9] B. Logan, J.M. Regan, Environ. Sci. Technol. 40 (17) (2006) 5172–5180.
[10] A. Meehan, H. Gao, Z. Lewandowski, IEEE Trans. Power Electron. 26 (1) (2011a) 176–181.
[11] W.S.D. Wilcock, P.C. Kauffman, J. Power Sources 66 (1–2) (1997) 71–75.
[12] S. Freguia, S. Tsujimura, K. Kano, Electrochim. Acta 55 (3) (2010) 813–818.
[13] Z. Wang, H. Deng, L. Chen, Y. Xiao, F. Zhao, Bioresour. Technol. 132 (2013a) 387–390.
[14] X. Xia, Y. Sun, P. Liang, X. Huang, Bioresour. Technol. 120 (2012) 26–33.
[15] P. Clauwaert, D. Van der Ha, N. Boon, K. Verbeken, M. Verhaege, K. Rabaey, W. Verstraete, Environ. Sci. Technol. 41 (21) (2007) 7564–7569.
[16] J.E. Kostka, A. Roychoudhury, P. Van Cappellen, Biogeochemistry 60 (1) (2002) 49–76.
[17] P. Sampou, C.A. Oviatt, Mar. Ecol. Prog. Ser. 72 (3) (1991) 271–282.
[18] J. Meng, Z. Xu, J. Guo, Y. Yue, X. Sun, PLoS ONE 8 (9) (2013) e73907.
[19] Y.C. Yong, Y.Y. Yu, C.M. Li, J.J. Zhong, H. Song, Biosens. Bioelectron. 30 (1) (2011) 87–92.
[20] A. Kumar, K. Katuri, P. Lens, D. Leech, Biochem. Soc. Trans. 40 (6) (2012) 1308–1314.
[21] B.M. Fonseca, C.M. Paquete, S.E. Neto, I. Pacheco, C.M. Soares, R.O. Louro, Biochem. J. 449 (1) (2013) 101–108.
[22] M. Miethke, Metallomics 5 (1) (2013) 15–28.

[23] L. Shi, K.M. Rosso, J.M. Zachara, J.K. Fredrickson, Biochem. Soc. Trans. 40 (6) (2012) 1261–1267.
[24] L. Morgado, A.P. Fernandes, J.M. Dantas, M.A. Silva, C.A. Salgueiro, Biochem. Soc. Trans. 40 (6) (2012) 1295–1301.
[25] Y. Ahn, M.C. Hatzell, F. Zhang, B.E. Logan, J. Power Sources 249 (2014) 440–445.
[26] T. Catal, D. Cysneiros, V. O'Flaherty, D. Leech, Bioresour. Technol. 102 (1) (2011) 404–410.
[27] Z. Du, H. Li, T. Gu, Biotechnol. Adv. 25 (5) (2007) 464–482.
[28] I. Durruty, P.S. Bonanni, J.F. Gonzalez, J.P. Busalmen, Bioresour. Technol. 105 (2012) 81–87.
[29] Y. Feng, X. Wang, B.E. Logan, H. Lee, Appl. Microbiol. Biotechnol. 78 (5) (2008) 873–880.
[30] S. Hays, F. Zhang, B.E. Logan, J. Power Sources 196 (20) (2011) 8293–8300.
[31] U. Karra, S.S. Manickam, J.R. McCutcheon, N. Patel, B. Li, Int. J. Hydrogen Energy 38 (3) (2013a) 1588–1597.
[32] U. Karra, E. Troop, M. Curtis, K. Scheible, C. Tenaglier, N. Patel, B. Li, Int. J. Hydrogen Energy 38 (13) (2013b) 5383–5388.
[33] X. Li, N. Zhu, Y. Wang, P. Li, P. Wu, J. Wu, Bioresour. Technol. 128 (2013) 454–460.
[34] H. Liu, S. Cheng, B.E. Logan, Environ. Sci. Technol. 39 (14) (2005a) 5488–5493.
[35] H. Liu, S.A. Cheng, B.E. Logan, Environ. Sci. Technol. 39 (2) (2005b) 658–662.
[36] B.E. Logan, K. Rabaey, Science 337 (6095) (2012) 686–690.
[37] N. Lu, S.G. Zhou, L. Zhuang, J.T. Zhang, J.R. Ni, Biochem. Eng. J. 43 (3) (2009) 246–251.
[38] P.L. McCarty, J. Bae, J. Kim, Environ. Sci. Technol. 45 (17) (2011) 7100–7106.
[39] B. Min, J. Kim, S. Oh, J.M. Regan, B.E. Logan, Water Res. 39 (20) (2005) 4961–4968.
[40] M. Miyahara, K. Hashimoto, K. Watanabe, J. Biosci. Bioeng. 115 (2) (2013) 176–181.
[41] D.H. Park, J.G. Zeikus, Appl. Environ. Microbiol. 66 (4) (2000) 1292–1297.
[42] M. Rahimnejad, A.A. Ghoreyshi, G. Najafpour, T. Jafary, Appl. Energy 88 (11) (2011) 3999–4004.
[43] S. Sevda, X. Dominguez-Benetton, K. Vanbroekhoven, H. De Wever, T.R. Sreekrishnan, D. Pant, Appl. Energy 105 (2013) 194–206.
[44] H. Wang, S.C. Jiang, Y. Wang, B. Xiao, Bioresour. Technol. 138 (2013b) 109–116.
[45] Y. Feng, W. He, J. Liu, X. Wang, Y. Qu, N. Ren, A horizontal plug flow and stackable pilot microbial fuel cell for municipal wastewater treatment, Bioresour. Technol. 156 (2014) 132–138.
[46] J. Winfield, I. Ieropoulos, J. Greenman, Bioresour. Technol. 110 (2012) 245–250.
[47] J. Yang, Y. Zhao, C. Zhang, Y. Hu, M. Zhou, Electrochem. Commun. 34 (2013) 121–124.
[48] C.P. Yu, Z. Liang, A. Das, Z. Hu, Water Res. 45 (3) (2011) 1157–1164.
[49] F. Zhang, Y. Ahn, B.E. Logan, Bioresour. Technol. 152 (2014) 46–52.
[50] S.J. Andersen, I. Pikaar, S. Freguia, B.C. Lovell, K. Rabaey, R.A. Rozendal, Environ. Sci. Technol. 47 (10) (2013) 5488–5494.
[51] A. Dewan, S.U. Ay, M.N. Karim, H. Beyenal, J. Power Sources 245 (2014) 129–143.
[52] C. Donovan, A. Dewan, D. Heo, H. Beyenal, Environ. Sci. Technol. 42 (22) (2008) 8591–8596.
[53] C. Donovan, A. Dewan, D. Heo, Z. Lewandowski, H. Beyenal, J. Power Sources 233 (2013) 79–85.
[54] C. Donovan, A. Dewan, H.A. Peng, D. Heo, H. Beyenal, J. Power Sources 196 (3) (2011) 1171–1177.
[55] Y. Gong, S.E. Radachowsky, M. Wolf, M.E. Nielsen, P.R. Girguis, C.E. Reimers, Environ. Sci. Technol. 45 (11) (2011) 5047–5053.
[56] J.D. Park, Z.Y. Ren, IEEE Trans. Energy Convers. 27 (3) (2012a) 715–724.
[57] J.D. Park, Z.Y. Ren, J. Power Sources 205 (2012b) 151–156.
[58] H. Wang, J.D. Park, Z. Ren, Environ. Sci. Technol. 46 (9) (2012) 5247–5252.
[59] F. Yang, D.X. Zhang, T. Shimotori, K.C. Wang, Y. Huang, J. Power Sources 205 (2012) 86–92.
[60] D.X. Zhang, F. Yang, T. Shimotori, K.C. Wang, Y. Huang, J. Power Sources 217 (2012) 65–71.
[61] F. Zhang, L. Tian, Z. He, J. Power Sources 196 (22) (2011) 9568–9573.
[62] E. Gavalakis, D. Mamais, C. Marinos, A.D. Andreadakis, Global Nest J. 8 (1) (2006) 75–81.
[63] A. Dewan, C. Donovan, D. Heo, H. Beyenal, J. Power Sources 195 (1) (2010) 90–96.
[64] Z. Lewandowski, H. Beyenal, Fundamentals of Biofilm Research, CRC Press, Boca Raton, FL, 2014.
[65] M. Yucel, Estuar. Coast. Shelf Sci. 131 (2013) 83–92.
[66] S. Rigaud, O. Radakovitch, R.M. Couture, B. Deflandre, D. Cossa, C. Garnier, J.M. Garnier, Appl. Geochem. 31 (2013) 35–51.
[67] A. Dewan, H. Beyenal, Z. Lewandowski, Environ. Sci. Technol. 42 (20) (2008) 7643–7648.
[68] D.Y. Huang, S.G. Zhou, Q. Chen, B. Zhao, Y. Yuan, L. Zhuang, Chem. Eng. J. 172 (2–3) (2011) 647–653.
[69] L. Huang, Q. Wang, X. Quan, Y. Liu, G. Chen, Bioelectrochemistry 94 (2013) 13–22.
[70] S. You, Q. Zhao, J. Zhang, J. Jiang, S. Zhao, J. Power Sources 162 (2) (2006) 1409–1415.
[71] S. You, Q. Zhao, J. Zhang, H. Liu, J. Jiang, S. Zhao, Biosens. Bioelectron. 23 (7) (2008) 1157–1160.
[72] J. Menicucci, H. Beyenal, E. Marsili, R.A. Veluchamy, G. Demir, Z. Lewandowski, Environ. Sci. Technol. 40 (3) (2006) 1062–1068.
[73] T. Huggins, P.H. Fallgren, S. Jin, Z.J. Ren, J. Microb. Biochem. Technol. S6 (2013).
[74] T. Huggins, P.H. Fallgren, J. Microb. Biochem. Technol. (2013).
[75] Center for Sustainable Systems, University of Michigan, 2013. U.S. Wastewater Treatment Factsheet. Pub. No. CSS04-14.